Src Regulates Actin Dynamics and Invasion of Malignant Glial Cells in Three Dimensions

Alexandre Angers-Loustau,[1] Ramm Hering,[1] Tamra E. Werbowetski,[1] David R. Kaplan,[1,2] and Rolando F. Del Maestro[1]

[1]Brain Tumor Research Center, Montreal Neurological Institute and Hospital, Department of Neurology and Neurosurgery, McGill University, Montreal, Quebec, Canada and [2]Hospital for Sick Children and Department of Molecular Genetics and Microbiology, University of Toronto, Toronto, Ontario, Canada

Abstract

Malignant glioma is the major brain tumor in adults and has a poor prognosis. The failure to control invasive cell subpopulations may be the key reason for local glioma recurrence after radical tumor resection and may contribute substantially to the failure of the other treatment modalities such as radiation therapy and chemotherapy. As a model for this invasion, we have implanted spheroids from a human glioma cell line (U251) in three-dimensional collagen type I matrices, which these cells readily invade. We first observed that the Src family kinase-specific pharmacologic inhibitors PP2 and SU6656 significantly inhibited the invasion of the cells in this assay. We confirmed this result by showing that expression of two inhibitors of Src family function, dominant-negative-Src and CSK, also suppressed glioma cell invasion. To characterize this effect at the level of the cytoskeleton, we used fluorescent time-lapse microscopy on U251 cells stably expressing a YFP-actin construct and observed a rapid change in actin dynamics following addition of PP2 in both two-dimensional and three-dimensional cultures. In monolayer cultures, PP2 caused the disappearance of peripheral membrane ruffles within minutes. In three-dimensional cultures, PP2 induced the loss of actin bursting at the leading tip of the invadopodium. The inhibition of Src family activity is thus a potential therapeutic approach to treat highly invasive malignant glioma. (Mol Cancer Res 2004;2(11):595–605)

Received 7/26/04; revised 9/15/04; accepted 9/27/04.

Grant support: Alex Pavanel and Franco Di Giovanni Funds for Brain Tumor Research (R.F. Del Maestro), Canadian Cancer Society and National Cancer Institute of Canada (D.R. Kaplan), National Cancer Institute of Canada Terry Fox Studentship (A. Angers-Loustau), Canadian Institute for Health Research doctoral research award (T.E. Werbowetski), Harold Johns and Canadian Cancer Society research scientist award and Canada Research Chair (D.R. Kaplan), Montreal Neurological Institute Killam Scholarship, and William Feindel Chair in Neuro-Oncology (R.F. Del Maestro).

The costs of publication of this article were defrayed in part by the payment of page charges. This article must therefore be hereby marked advertisement in accordance with 18 U.S.C. Section 1734 solely to indicate this fact.

Note: A. Angers-Loustau was cosupervised by R.F. Del Maestro and D.R. Kaplan.

Requests for reprints: Rolando Del Maestro, Brain Tumor Research Center, Montreal Neurological Institute and Hospital, Department of Neurology and Neurosurgery, McGill University, 3801 University Room BT-205, Montreal, Quebec, Canada H3A 2B4. Phone: 514-398-8293; Fax: 514-398-3971. E-mail: rolando.delmaestro@mcgill.ca

Introduction

Grade IV astrocytoma or glioblastoma multiforme is distinct in that it rarely metastasizes outside the brain (reviewed in ref. 1). However, despite the advances in surgical and radiotherapy techniques and the development of new chemotherapeutic regimens and reagents, patient prognosis remains poor. This is due to the presence in glioblastoma multiforme of subpopulations of highly invasive cells that disseminate into the surrounding brain parenchyma and result in tumor recurrence at the edges of the resection cavity and/or at distant sites in the brain.

In our attempts to characterize the determinants of glioma cell invasion, we have developed and characterized a model where glioma cell aggregates are implanted in a solid collagen type I matrix (2-4). This method approximates the *in vivo* environment of tumor invasion more accurately than standard two-dimensional migration assays while allowing for convenient monitoring of invasion rates and individual cell behavior (5). The benefits of three-dimensional systems have become evident in light of recent observations concerning the difference in behavior between cells migrating on a two-dimensional plane and cells invading a matrix (6-8). Strategies that efficiently impair migration in monolayers have been ineffective when used to modulate invasion due to the capacity of these cells to adapt their behavior and continue their ability to invade.

The three-dimensional matrix model system can be readily manipulated by addition of different soluble reagents in the matrix; we have therefore used this system to assess the ability of available pharmacological agents to inhibit glioma invasion.[3] We found that among the most effective agents that decreased the invasion rates of glioma cells were the Src family kinase inhibitors PP2 and SU6656. We confirmed these results by showing that expression of two inhibitors of Src family function, dominant-negative (DN)-Src and CSK, also suppressed glioma cell invasion. In monolayer cultures, addition of PP2 resulted in the rapid and selective disappearance of peripheral membrane ruffles. This seems to correspond in the three-dimensional collagen matrix to a loss of actin bursting activity at the tip of the invadopodia. Taken together, these results suggest that Src protein kinases are involved in glioma cell invasion by regulating actin dynamics.

[3] R. Hering et al., submitted for publication.

Results

Inhibition of Glioma Cell Invasion in Three Dimensions by Src Inhibitors

Src inhibitors have been shown to suppress the invasion of prostate, colon, and ovarian cancer cells (9-11). Similarly, our screen of inhibitors of glioma invasion in three-dimensional matrices indicated that among the most effective inhibitory agents was the Src family kinase inhibitor PP2. When spheroids of the human glioma cell line U251 were implanted into the collagen gel, the cells rapidly invaded the matrix radially and the extent of invasion can be assessed by measuring the diameter between the fronts of invading cells. Addition of the Src family kinase inhibitor PP2 to the medium inhibited this invasion in a dose-dependent manner (Fig. 1A). PP3, an analogue of PP2, was used as a negative control because it exhibits the same nonspecific effects as PP2 without inhibiting the Src family kinases (12, 13). In our assay, PP3 did not significantly alter the invasion of the U251 cells from the spheroid into the collagen matrix even at high concentrations (Fig. 1A). Similar results were obtained with PP2 and PP3 using spheroids of C6 astrocytoma rat cells, showing that this effect is not specific to the U251 human glioma cells (data not shown).

One concern of using PP2 is that it also inhibits the kinase activity of the platelet-derived growth factor receptor, which is overexpressed in glioma tumors (14). To confirm that the effect on glioma invasion was due to the suppression of Src family kinase activity and not platelet-derived growth factor receptor activity, we used the inhibitor SU6656, which was originally selected for its specificity toward Src and its lack of effect on the platelet-derived growth factor receptor (15). Figure 1B shows that SU6656 significantly decreased the extent of glioma cell invasion into the three-dimensional collagen matrix, strongly suggesting that the suppression of invasion is due to Src family kinase inhibition.

To confirm that the effect of PP2 on tumor cell invasion was at the level of the rate of cell movement, we measured the rate of invasion of individual cells into the collagen matrix using time-lapse videomicroscopy. U251 spheroids were implanted into three-dimensional collagen gels and allowed to invade so that individual invading cells at a distance from the main spheroid mass could be identified and monitored. At 24 hours postimplantation, the gel was overlaid with either medium or medium containing 10 μmol/L PP2 and placed into a chamber attached to a microscope. A computer-controlled camera was used to take bright-field pictures of the invading cells every 4 minutes for 24 hours. After this time, a video was generated, which allowed the tracing of the invasion paths of each of the cells from the commencement of invasion. The distances

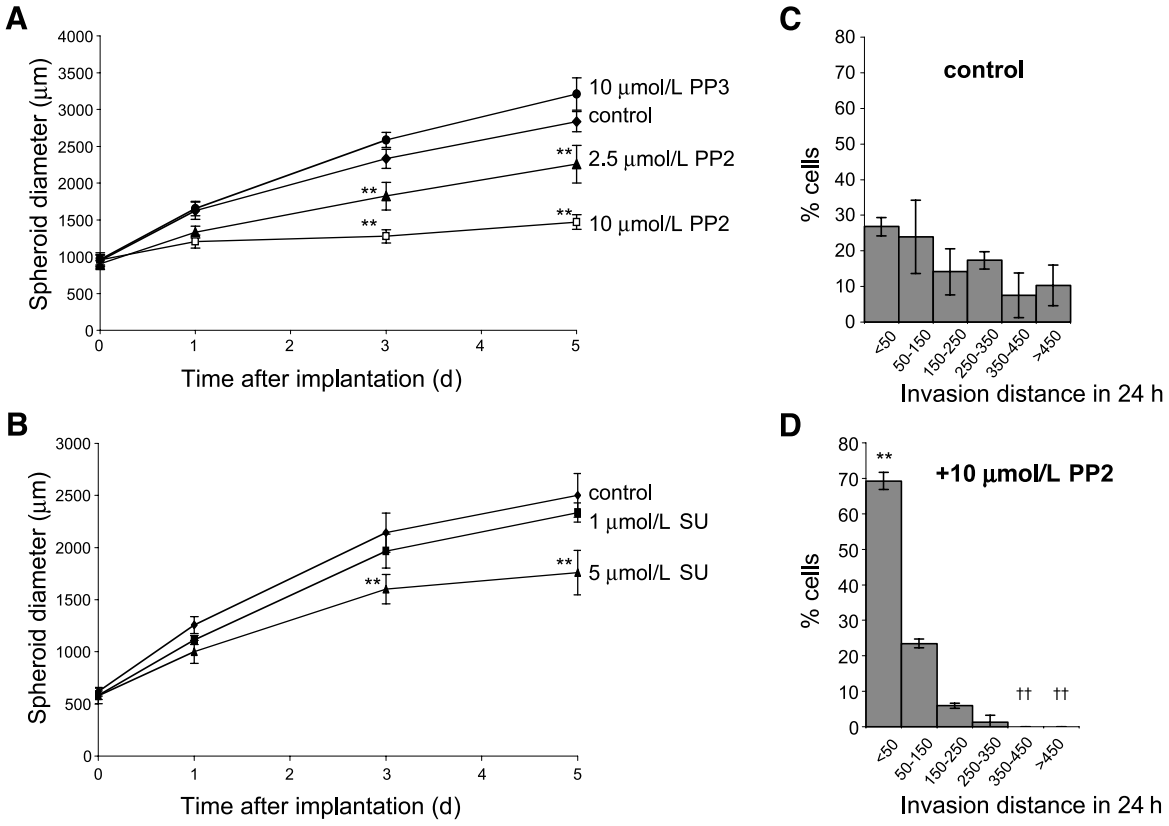

FIGURE 1. Effects of the Src inhibitors on glioma invasion. **A.** Dose-dependent decrease in the invasion of U251 spheroids in a three-dimensional collagen matrix with PP2 but not with PP3 (n = 8 spheroids per condition). **, $P < 0.01$, compared with control (two-factor mixed-design ANOVA). **B.** Similar effect observed with SU6566 (*SU*). **C.** Single-cell invasion distances of U251 glioma cells between 24 and 48 hours after implantation measured using time-lapse videomicroscopy. Measurements were separated in 100 μm intervals. *Bars,* % cells whose invasion distance fell within that interval in each experiment. **D.** Effect of addition in the matrix of 10 μmol/L PP2 on the distribution seen in **C**. The great majority of the cells (70%) do not invade >50 μm in that interval (n = 3 movies, an average of 40 cells measured for each). **, $P < 0.01$, significantly higher than control; ††, $P < 0.01$, significantly lower than control.

calculated using the Northern Eclipse program are shown in Fig. 1C and D. The results are shown as a distribution of cells invading different distance intervals. In normal conditions (Fig. 1C), some cells invade very little or not at all (<50 μm) in the period assessed, whereas others invade large distances in the same period (>450 μm). Addition of 10 μmol/L PP2 caused a significant shift of the distribution toward small invasion distances (Fig. 1D), confirming that the inhibition of the tumor spread observed in Fig. 1A is due to a reduction of the cell invasion velocity into the collagen matrix. However, these results do not detect the effects of Src inhibition in the percentage of glioma cells participating in invasion, because only the cells that detached from the spheroid after the first 24 hours, when no inhibitors are present, are measured.

The Src inhibitors used in this study inhibit all of the Src family kinases. Three of these kinases, Src, Fyn, and Yes, were expressed in glioma cells as shown by probing lysates of U251 cells with antibodies to these proteins (Fig. 2A, *top*, and B). c-Src also has a neuronal-specific splice form (N-Src), which contains an insert of 6 amino acids. To determine which Src protein was expressed in U251 cells, we generated a N-Src-specific antibody by immunizing rabbits with a polypeptide composed of the 6 N-Src-specific amino acids. The resulting antibody specifically immunoprecipitated N-Src (data not shown). Lysates from U251 cells were immunoprecipitated with anti-N-Src and probed in Western blots with an antibody that recognizes both c-Src and N-Src. Figure 2A shows that U251 cells express c-Src (*top*) but not N-Src (*bottom*). As controls, human 293 cells, which express c-Src, and a fragment of human normal cortex obtained from a surgical operation, which expresses N-Src, are shown. The significance of this absence of N-Src from glioma and the expression patterns of this splice form in different populations of neural stem cells (see ref. 16) and different stages of differentiation are currently under investigation. Taken together, those results indicate that the targets of our inhibitors are expressed in the cell line used.

To confirm that the PP2 inhibitor used in our studies was able to efficiently inhibit c-Src activity in the U251 glioma cell, we tested its ability to block the tyrosine phosphorylation induced by activated Src (Src Y527F; see ref. 17). U251 cells were infected with recombinant adenoviruses expressing activated Src and treated with different amounts of PP2. After 24 hours, the cells were harvested and the phosphotyrosine pattern in the total cell lysate was evaluated with anti-phosphotyrosine. Figure 2C shows that PP2 is able to efficiently block c-Src activity even when the enzyme is in an activated conformation. However, we could not assess whether PP2 suppressed the activity of endogenous Src due to the low detectable basal *in vitro* kinase activity of Src in U251 cells.

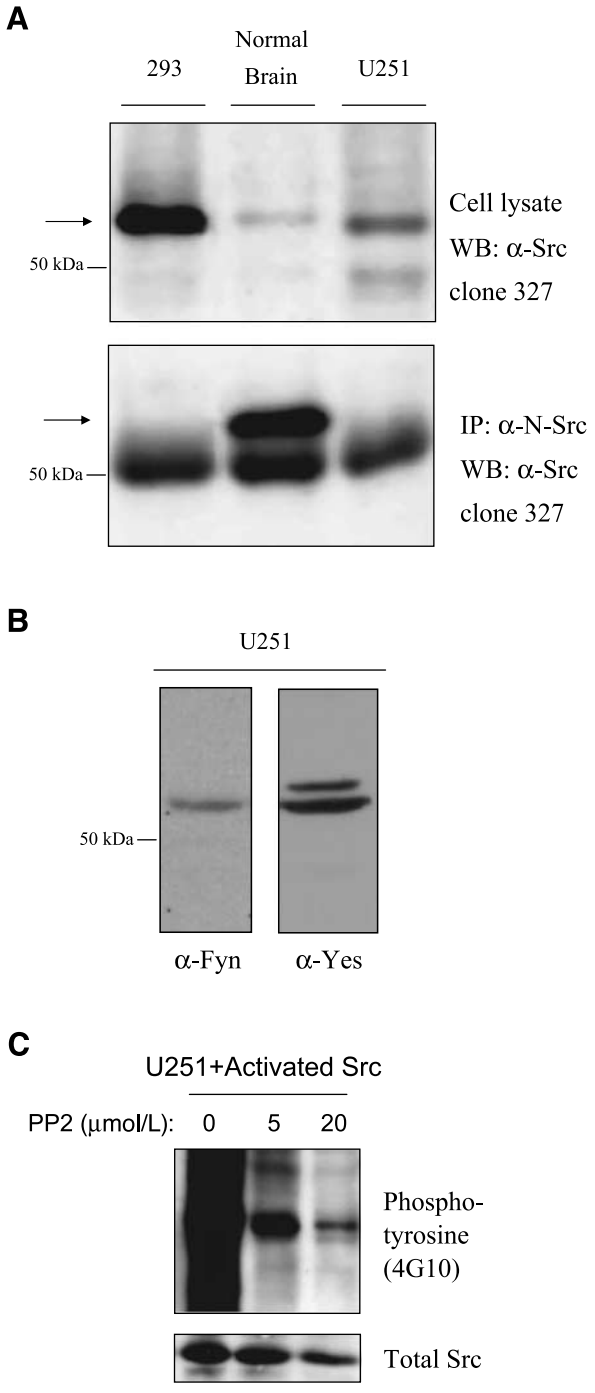

FIGURE 2. U251 glioma cells express Src, Fyn, and Yes but not N-Src. **A.** Western blot (*WB*) of total cell lysates obtained from 293 cells, normal human brain, and U251 cells probed for Src (*top*). Immunoprecipitation (*IP*) of the same lysates using a N-Src-specific antibody probed with the Src antibody, which recognizes both N-Src and c-Src, showing that N-Src is expressed in normal human brain but not in the human glioblastoma cell line U251 (*bottom*). **B.** Western blot of total cell lysate from U251 cells probed for Yes and Fyn antibodies. **C.** Efficient inhibition of Src activity by the inhibitor PP2. Total cell lysates of U251 cells expressing activated Src were probed with an anti-phosphotyrosine antibody to confirm the disappearance of the signal when increasing concentrations of PP2 are added.

PP2 Decreases the Proliferation Rate of Glioma Cells

We then asked whether the inhibition of glioma invasion by PP2 was due to a toxic or apoptotic effect of the Src inhibitor on the tumor cells. U251 cells grown in monolayers were trypsinized, counted, and plated in six-well plates (day 0). At day 1, cells were treated with 10 μmol/L PP2 or 5 μmol/L SU6656 and the cells were counted every 2 days. Figure 3A shows a significant decrease in the proliferation rates of glioma cells following treatment with PP2 or SU6656. The calculated

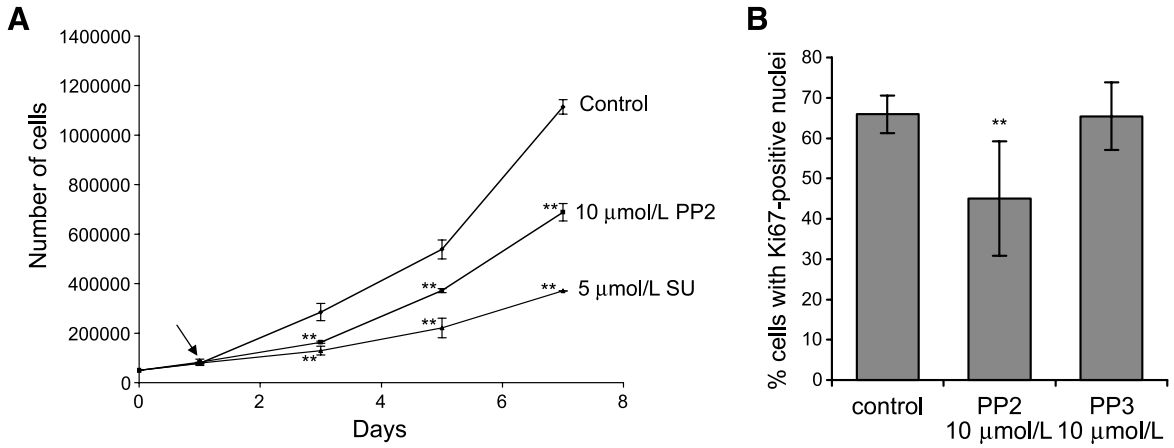

FIGURE 3. Effects of PP2 on U251 glioma cells proliferation. **A.** Decrease in the proliferation rates of glioma cells by PP2 and SU6656. At *day 0*, 50,000 cells were plated in six-well plates and the inhibitors were added at *day 1* (*arrow*). Cells were counted every 2 days by trypsinizing the cells and feeding them in a Coulter particle counter. **, $P < 0.01$, compared with control (two-factor ANOVA). **B.** Decrease in the proliferation index of the cultures with PP2 but not with PP3 as measured by the ratio of Ki67-positive nuclei 4 days after addition of the inhibitors. **, $P < 0.01$, compared with control (ANOVA).

doubling times of the cultures were 36, 44, and 60 hours for control, PP2-treated, and SU6656-treated cells, respectively. During the proliferation assay, no significant cell death or de-adhesion was observed (data not shown). In addition, when the cells were labeled with terminal deoxynucleotidyl transferase dUTP nick end labeling, which stains apoptotic nuclei, <3% of both control and treated cells showed staining within their nuclei (data not shown), indicating that the decrease in the number of cells treated with the Src inhibitor was not due to cell death.

We then examined the effect of PP2 on glioma cell proliferation by indirect immunofluorescence with anti-Ki67, a protein found in the nuclei of proliferating cells (18). Cells were treated with PP2 or PP3 for 4 days, fixed, and stained and the percentage of proliferating cells was counted in random fields. Figure 3B shows a decreased proliferation index in glioma cell cultures treated with 10 μmol/L PP2 but not with PP3, suggesting that inhibition of Src family kinase activity in glioma cells results in an exit from the cell cycle in monolayers. It is highly probable that Src inhibition can cause similar effects on the proliferation of glioma cells invading three-dimensional matrices, which may contribute to the decrease in the extent of spheroid spread observed in Fig. 1A.

Overexpression of DN-Src and CSK Decreases the Invasion Rates of Individual Glioma Cells

To confirm the role of Src in regulating the rate of glioma invasion, we expressed two inhibitors of Src family function, DN c-Src and CSK, in U251 cells. The DN-Src mutant used encodes two mutations, lysine to arginine at amino acid 255 and tyrosine to phenylalanine at position 527, that renders the enzyme catalytically inactive and locked in an open conformation and effective in sequestering Src family kinase activators and substrates, therefore interfering with the activity of all Src family members. CSK phosphorylates Src, Fyn, and Yes on a COOH-terminal tyrosine, inactivating those enzymes (19). To express DN-Src and CSK in glioma cells, we cloned the genes encoding these proteins into recombinant adenovirus vectors, which we showed previously allows efficient and nontoxic expression of genes in glioma cell lines (20). The adenovirus vector used, pAdTrack, also expresses the green fluorescent protein (GFP) on a separate cytomegalovirus promoter, which allows for identification of the infected cells.

U251 spheroids were incubated in suspension with the recombinant adenoviruses prior to implantation. During the first 24 hours, the cells invaded the matrix; after that time, infected cells commenced expressing the recombinant gene products. This method eliminates the possible effects of adenoviral infection on spheroid formation or cell detachment from the main tumor mass. The cells were then filmed during the second 24 hours and their individual invasion distances were assessed. Once the distances were recorded, a GFP fluorescence image was overlaid on the first image of migrating cells to identify which cells expressed DN-Src/GFP, CSK/GFP, or GFP. Because we routinely infect ~50% of the cells in a spheroid, the uninfected cells provide an internal control for each experiment.

In cells expressing GFP alone, no significant effect on invasion was observed as compared with noninfected cells in the same spheroid (Fig. 4A). In contrast, expression of DN-Src or CSK significantly reduced the invasion distances of the cells (Fig. 4B and C), confirming that the results obtained with PP2 and SU6656 were indeed due to inhibition of Src family member activity. These results as well as the results from Fig. 1C and D are summarized in Table 1. Table 1 also shows the maximum invasion distance for an individual cell observed in all the conditions. Treatment of cells with PP2 as well as overexpression of DN-Src or CSK not only resulted in a significant decrease in the average invasion distances of the glioma cells in the three-dimensional collagen matrix but also eliminated the subpopulation of the most highly invasive cells.

Src Inhibition Causes a Rapid Disappearance of Lamellipodia in Glioma Cells in Two Dimensions

Src tyrosine kinases have been linked to the regulation of cell adhesion (21). For example, src−/− fibroblasts obtained

from gene targeting in mice showed an impairment in spreading and adhesion on fibronectin substrates (22). Src was also found to have a role in the regulation of actin dynamics (23, 24) and to be involved in tumor cell invasion at the level of extracellular matrix degradation (9, 11). To examine how Src regulates glioma cell invasion, we tested the effects of the Src inhibitors on the cytoskeletal dynamics within live cells. To perform this study, we first generated U251 cell lines that stably expressed a YFP-tagged actin protein. This fusion protein becomes incorporated in the actin fibers forming different structures within the cells, and their dynamics can be monitored in live cells using time-lapse fluorescent microscopy (25).

Figure 5A shows one of the YFP-actin expressing cells grown in a monolayer. Different structures can be seen, such as stress fibers and a large lamellipodium at the leading front of the cell (*arrow*). After addition of 10 μmol/L PP2, we observed within minutes the rapid disappearance of the lamellipodium. This loss was selective and not due to general actin disassembly because stress fibers did not disappear even after longer periods (data not shown). To quantify this effect and to confirm that this was not due to aberrant effects of overexpressing YFP-actin, the disappearance of actin-rich ruffles was measured after PP2 treatment of U251 cells. Under phase microscopy, the ruffles appear as dark borders at the cell periphery (Fig. 5B, *arrows*). Cells were counted as "ruffle positive" if they contained at least one of these ruffles. At time 0, PP2 was added to a final

Table 1. Summary of the Mean and Maximum Distances (μm) Obtained in Figs. 1C and D and 4

	Mean ± SD Invasion (μm)	Maximum Invasion (μm)	*P*
Control (n = 281)	198 ± 192	884	
PP2 (10 μmol/L, n = 68)	43 ± 60	333	<0.01
Ad-GFP (n = 82)	175 ± 174	771	NS
Ad-DN-Src (n = 30)	44 ± 60	250	<0.01
Ad-CSK (n = 44)	90 ± 85	323	<0.01

NOTE: Maximum invasion represents the furthest distance recorded for a single cell in the invading population for a 24-hour period. *P*s refer to the comparison of the mean invasion values by ANOVA. See text for details.

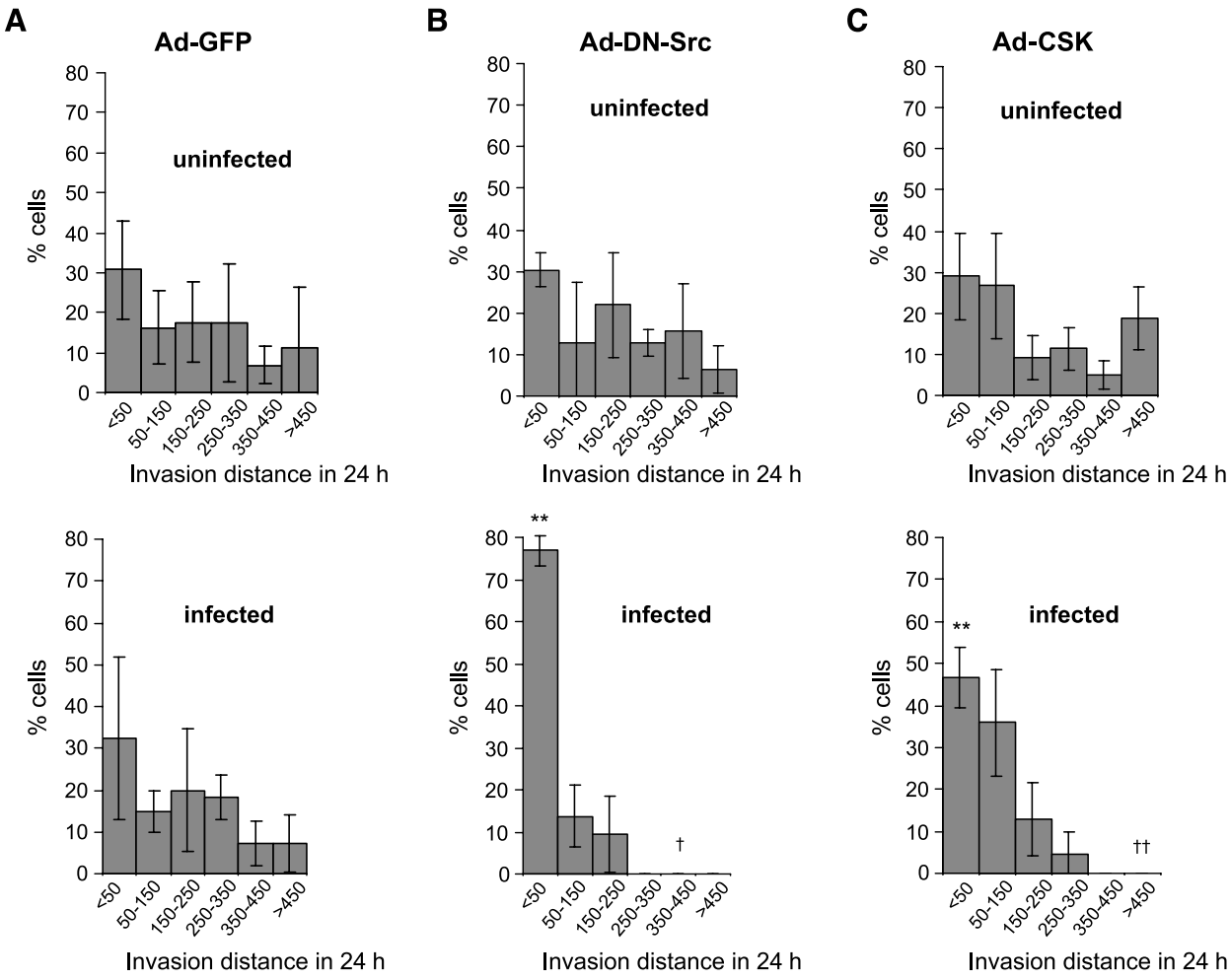

FIGURE 4. Expression of DN-Src and CSK in the cells invading the collagen matrix. **A.** Infection of the cells with a GFP-expressing adenovirus (*bottom*) did not significantly alter their invasion velocity compared with control, noninfected cells in the same spheroids (*top*). **B.** Expression of a DN mutant of c-Src significantly decreased U251 invasion distances. **C.** Expression of CSK also, to a lesser extent, shifted the distribution toward smaller invasion distances (n = 3 movies, an average of 20 cells measured for each). **, $P < 0.01$, significantly higher than control; †, $P < 0.05$; ††, $P < 0.01$, significantly lower than control.

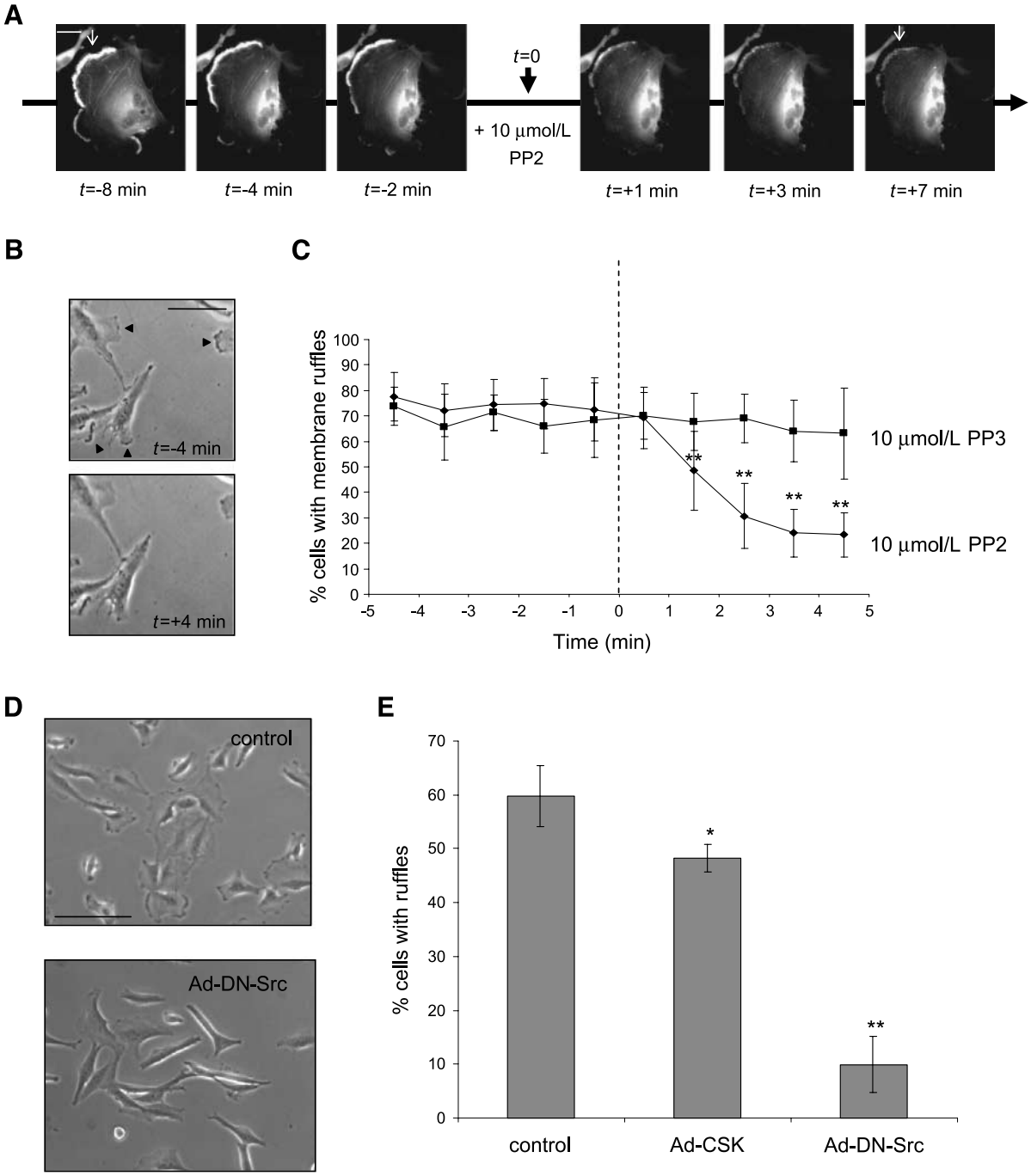

FIGURE 5. Effect of PP2 on peripheral membrane ruffles in glioma cells. **A.** Fluorescent time-lapse videomicroscopy images of a single U251 stably expressing a YFP-actin construct before and after addition of 10 μmol/L PP2 show a selective disappearance of the peripheral membrane ruffle (*arrow*). *Bar*, 20 μm. **B** and **C.** Quantification of this effect using low-magnification time-lapse videomicroscopy of untransfected U251 cells. Under phase, the peripheral lamellipodia appear as phase-dark ruffles (*arrows*) and disappear after addition of PP2 (**B**). *Bar*, 50 μm. Quantification shows that this effect is specific to PP2 and becomes significant 2 minutes after addition of PP2 at *time 0* ($n = 8$ movies, an average of 40 cells counted for each). **, $P < 0.01$ compared with PP3 (two-factor mixed-design ANOVA). **D** and **E.** Effects of the recombinant adenoviruses on the number of cells with membrane ruffles in the population ($n = 3$, an average of 95 cells counted for each). *, $P < 0.05$; **, $P < 0.01$, compared with control (ANOVA). Images show typical fields 24 hours after addition of the virus. *Bar*, 50 μm.

concentration of 5 μmol/L. Figure 5C shows the rapid decrease in ruffle-positive cells in the population that becomes significant after ~1 minute of PP2 addition (5 μmol/L). A similar effect was observed with SU6656 (data not shown). To confirm that this is not a response of the cells to fluid perturbation caused by the addition of PP2 to the culture, the same experiment was repeated without inhibitor (data not shown) or the negative control PP3 with no effect observed (Fig. 5C).

This loss of lamellipodia following PP2 treatment was confirmed using the recombinant DN-Src and CSK adenoviruses. Low confluency monolayers of U251 cells were infected with the DN-Src and CSK viruses at a multiplicity of infection sufficient to infect 100% of the cells with no evident toxicity. Twenty-four hours after infection, random phase-contrast fields were photographed and the percentage of cells containing membrane ruffles was counted for each condition. Figure 5D shows that U251 cells infected with DN-Src exhibited significantly reduced cell ruffling and adopted an elongated morphology. Quantification of this phenotype shows that DN-Src and, to a much lesser extent, CSK significantly decreased the number of cells containing membrane ruffles in the population (Fig. 5E).

PP2 Causes a Rapid Loss of Actin Bursting at the Invading Tip of U251 Cells in Three Dimensions

We then analyze whether the loss of lamellipodia observed in monolayer cultures treated with PP2 similarly affected actin

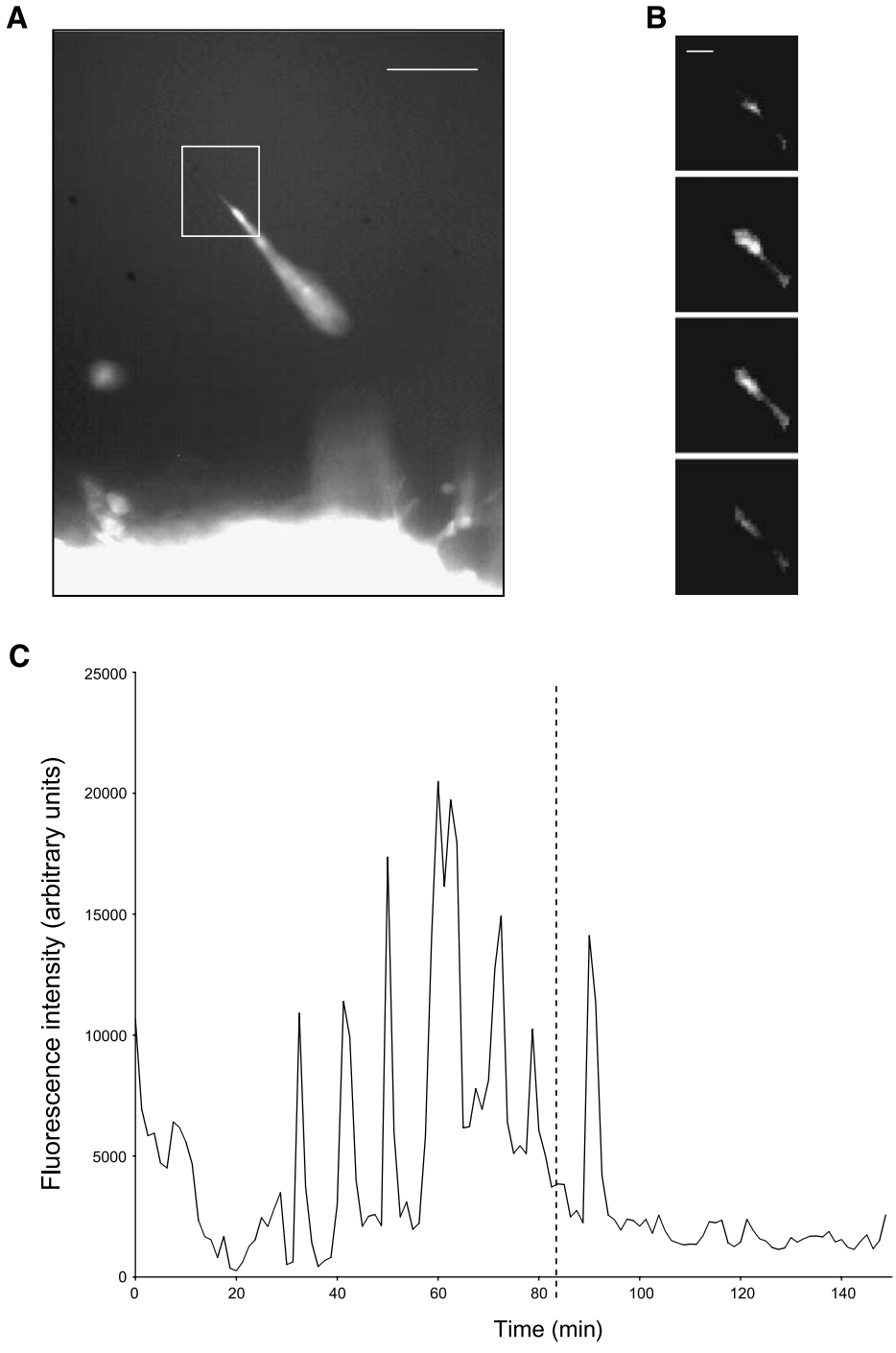

FIGURE 6. Effect of PP2 on the actin dynamics in U251 in the three-dimensional collagen matrix. **A.** YFP-actin image of a cell invading away from the spheroid (*bottom*). *Bar*, 20 μm. **B.** High-magnification zoom of the invading tip of the cell showing a "burst" of actin. *Bar*, 2 μm. **C.** Quantification of the fluorescence intensity in the area in **A** shows that this bursting occurs at regular interval in this cell and is abrogated by the addition of 5 μmol/L PP2 on the collagen gel (*dashed line*).

dynamics in cells invading a three-dimensional matrix. Spheroids from the YFP-actin–overexpressing U251 cells were generated and implanted into solid collagen matrices. After 24 hours, cell invasion by randomly invading cells was quantified by time-lapse fluorescent microscopy. These cells adopted a different morphology compared with the same cells grown in monolayers, exhibiting rounded cell bodies and long protrusions extending away from the main tumor mass (Fig. 6A). As in Fig. 5A, the same cells were monitored before and after the addition of PP2. Cells in the three-dimensional matrix did not form long membrane ruffles, but a close-up of the tip of the invadopodium revealed the presence of pulsating bursts of actin (Fig. 6B). Quantification of the fluorescence in this region shows that this bursting occurred at a regular frequency (every 10 minutes for this particular cell) and disappeared shortly after addition of 5 μmol/L PP2 (Fig. 6C).

Discussion

The ubiquitously expressed protein kinase Src has been implicated in numerous intracellular signal transduction pathways, which are important for tumor biology (see refs. 26-28 for recent reviews). Its involvement in cell migration made it an interesting potential target for the management of malignant glioma, whose poor prognosis can be linked to the invasive nature of the cells. Here, we show that inhibition of Src family kinase activity in the human glioblastoma cell line U251 resulted in reduced invasion velocities in a collagen matrix (Fig. 1). We have also shown that the three-dimensional invasion system can be adapted to study the effects of exogenously expressed proteins using adenoviral vectors (Fig. 4) as well as intracellular actin dynamics using YFP-tagged actin-expressing cells (Fig. 6).

To obtain these results, we have implanted glioma spheroids in three-dimensional collagen matrices. This model was chosen because it reflects many of the characteristics of glioma invasion of normal neural tissue *in vivo*, such as process extension, probing, degradation of the extracellular matrix, and adhesion to and detachment of the cell from the matrix. Collagen type I was chosen for its capacity to form solid gels at 37°C, which is not the case for other matrix components such as collagen type IV (4). The resulting matrix is free of growth factors and other types of extracellular components that could influence our experiments. Addition of other components to the matrix-like fibronectin or laminin, for example, had little effect on glioma invasion in this system and was not included here (4). An environment more similar to the situation encountered by glioma cells *in vivo* could be obtained by coculturing the glioma spheroids with rat brain aggregates (29-32). However, this type of experiment does not allow for the live qualitative and quantitative analysis of single invading glioma cells and will be part of future experiments designed to test the efficiency of Src inhibition on the control of glioma infiltration *in vivo*.

The involvement of Src in cell migration has led to recent interest in investigating the potential of Src as a target to block invasion in different types of cancer. Stable overexpression of DN-Src or CSK in carcinoma cells greatly decreased the potential of those cells to metastasize *in vivo* (33). In prostate cancer cells, invasion has been shown to correlate with FAK/Src signaling (34). The invasion of these cells was blocked by PP2 (34) as well as two novel Src inhibitors, CGP77675 and CGP76030 (10). The latter inhibitors were also shown to decrease proliferation of prostate cancer cells. In colon cancer cells, PP2 minimally affected proliferation but strongly inhibited invasion (11). Ovarian cancer cell invasion was also inhibited by addition of PP2 (9). In the case of colon and ovarian cancer cells, PP2 was shown to exert its effects at the level of extracellular matrix degradation by blocking urokinase-type plasminogen activator receptor expression (11) or transforming growth factor-β–induced urokinase-type plasminogen activator expression (9), respectively. Although we did not investigate these pathways in our glioma cells, time-lapse microscopy studies have shown effects of Src inhibition on glioma cell invasion at the level of peripheral actin dynamics (Figs. 5 and 6). Recent literature suggests potential targets for Src in these events. The small G-protein Rac, for example, has been long implicated in lamellipodia regulation (35). Src, by phosphorylating its substrate p130cas, creates binding sites for the protein Crk (36), which then recruits DOCK180, a member of a novel family of proteins that directly activate Rac (37, 38). However, we have shown recently that in glioma cells Rac is an important survival-inducing protein and that inhibition of its activity results in apoptosis of most glioblastoma cell lines and primary cells derived from human tumor samples (20). Another interesting candidate for a Src substrate affecting invasion is the F-actin binding cortactin. Phosphorylation of cortactin by Src is required for the formation of sphingosine-1-phosphate–induced membrane ruffling, and this effect is independent of Rac (24). In NIH-3T3 cells, expression of an inhibiting truncation of the Cbl proto-oncogene resulted in the formation of dorsal membrane ruffles that were also blocked by the PP2 inhibitor (39). Interestingly, unlike what we showed in Fig. 5 for U251 cells, PP2 did not inhibit the formation of peripheral actin ruffles in this system. We are currently characterizing the Src invasion pathway and particularly investigating whether other proteins that we have found to mediate glioma invasion such as Rho kinase (ROCK) are regulated by Src activity.

Our results suggest that in glioma cells Src is not mutated to become constitutively active. Indeed, CSK, which inhibits the activity of wild-type but not oncogenic Src, mimicked to some extent the effects of the Src inhibitors and DN-Src and suggests that the endogenous Src regulatory mechanisms are still functional. However, we could not determine whether the endogenous Src was hyperactivated in glioma cells, as the basal activity of the Src family members was difficult to detect. Src family activity may be concentrated in a subset of glioma cells (e.g., the most invasive cells) or elevated at the leading edge of those cells.

Several groups have suggested that, because cells use similar intracellular processes to migrate and to divide, inhibition of one process would result in an increase of the other (“Go or Grow” hypothesis; refs. 40-42). We have shown recently that this hypothesis does not describe the behavior of individual medulloblastoma cells in two-dimensional or three-dimensional collagen matrix invasion models (7). Recent data have also shown that targeting of one of these pathways in glioma cells does not necessarily result in overactivation of the other

(43, 44). Here, we show that inhibition of Src kinases results in a decrease of both glioma cell proliferation (Fig. 3) and invasion (Fig. 1). The effect of Src inhibition on the cell cycle might therefore be of concern if the Src inhibitors are used to treat glioma together with chemotherapeutic agents that depend on inducing cytotoxicity of proliferating cells. In addition, it is not known what the effect of Src inhibition is on non-transformed human astrocytes, although PP2 can inhibit the proliferation of normal rodent astrocytes (45).

The future treatment of high-grade glioma will depend on the ability of treatment modalities to target the highly infiltrative cells that escape surgical resection of the main tumor mass (46), whether by manipulating their survival (20, 47, 48), their extracellular guidance cues (29), or their intracellular invasion machinery (44, 49).[4] The three-dimensional collagen type I matrix has shown to predict, to some extent, the invasion of glioma cells into fetal and adult astrocytes aggregates (29) while allowing for the identification and characterization of proteins and agents that suppress invasion. We propose, based on our results using the three-dimensional collagen matrix, that Src inhibition following surgical removal of malignant glioma is a potential therapeutic avenue to prevent reoccurrence of this tumor.

Materials and Methods

Cell Culture

The human glioblastoma cell line U251 and the rat astrocytoma cell line C6 were purchased from American Type Culture Collection (Rockville, MD) and maintained in DMEM supplemented with 10% fetal bovine serum and penicillin/streptomycin in a humidified 37°C incubator containing 5% CO_2. A sample of normal human cortex was obtained from a surgical specimen (resected for tumor exposure) at the Montreal Neurological Institute and Hospital following guidelines.

Hanging drop aggregates were prepared as described previously (5, 7, 50). Briefly, 20 μL drops of DMEM/10% fetal bovine serum containing 30,000 cells each were deposited on the lid of a 100 mm Petri dish. The lid was then inverted and placed in the incubator for 3 days. The aggregates are then transferred into another dish coated with 2% agar in normal DMEM for 2 days.

Three-Dimensional Collagen Matrices

The glioma spheroids were implanted into three-dimensional collagen gels as described previously (4, 7). Briefly, a liquid bovine type I dermal collagen solution (3.0 mg/mL, Cohesion, Palo Alto, CA) was supplemented with one-tenth volume of 10 × DMEM. The pH of the solution was adjusted to 7.4 using 0.1 mol/L NaOH. This collagen preparation was aliquoted into 24-well plates (500 μL/well) and a glioma spheroid was added in each well while the solution was still viscous. The gel was solidified by incubating the plates at 37°C for 30 minutes before being overlaid with 500 μL of supplemented DMEM with or without pharmacologic inhibitors. If an inhibitor was added, its concentration was doubled in the overlay solution to take into account the volume of the gel. The Src inhibitors used (PP2, PP3, and SU6656) were purchased from Calbiochem (San Diego, CA) and resuspended in DMSO to a final concentration of 10 mmol/L. The extent of cell dispersion was measured every 2 days using a calibrated micrometer in the ocular of an inverted light microscope (5).

Single-Cell Invasion Distance Measurements

U251 spheroids were implanted as described above and allowed to invade for 24 hours. The plate was then placed in an inverted Axiovert 25 microscope (Carl Zeiss, Kirkland, Quebec, Canada) equipped with an environment chamber where temperature and CO_2 content were maintained by a heated stage and a CO_2 monitor (Carl Zeiss). Images of the invading cells were captured every 4 minutes for the next 24 hours by a Retiga 1300 CCD digital camera (Qimaging, Vancouver, British Columbia, Canada) controlled by the Northern Eclipse 6.0 time-lapse videomicroscopy software (Empix Imaging, Mississauga, Ontario, Canada). The individual images were then compiled into a movie (7). Every individual cell that detached from the main spheroid mass after the first 24 hours was numbered and their individual paths were traced on the screen by following them throughout the movie. The resulting traces were then measured using a calibrated Curve Measurement feature in the Northern Eclipse software. For measurements in the presence of PP2, the inhibitor was added a few minutes before starting the capture of the images.

Immunoprecipitation and Western Blotting

The c-Src antibody (clone 327) has been provided generously by Dr. Joanne Brugge (Harvard Medical School, Boston, MA). The rabbit polyclonal anti-Yes antibody was purchased from Upstate (Charlottesville, VA), whereas the mouse monoclonal anti-Fyn antibody was from Santa Cruz Biotechnology (Santa Cruz, CA). The N-Src-specific polyclonal antibody was generated by injecting rabbits with a synthetic peptide composed of residues NNTRKVDVREGD, the 6 amino acids specific to N-Src plus 3 amino acids on each side to help antigenicity, coupled to MA-peptide. For immunoprecipitation, cells or frozen tissue sample were lysed in radioimmunoprecipitation assay buffer [50 mmol/L Tris-HCl (pH 7.2), 150 mmol/L NaCl, 0.1% SDS, 0.5% sodium deoxycholate, 1% NP40]. The lysate was incubated with 4 μL of the N-Src-immunized whole rabbit serum and 30 μL of protein A-Sepharose (Amersham Biosciences, Piscataway, NJ) for 90 minutes at 4°C. The beads were washed three times with radioimmunoprecipitation assay buffer and resuspended in SDS-PAGE loading dye. Western blots were done following common procedures. The proteins were subjected to SDS-PAGE and transferred to nitrocellulose membranes. The membranes were blocked [150 mmol/L NaCl, 25 mmol/L Tris (pH 8.1), 5% milk, 0.05% Triton X-100] and incubated with the respective primary antibodies. The horseradish peroxidase–conjugated antibodies (Bio-Rad, Hercules, CA) were used at a 1:5,000 dilution and detected by chemiluminescence.

The PP2 inhibitor was tested by infecting U251 cells with activated Src-expressing adenoviruses (see below). At the time

[4] Hering et al., submitted for publication.

of infection, different concentrations of the inhibitor was added to the supernatant. At 24 hours postinfection, the cells were harvested and lysed as described above and the total cell lysate was probed with the anti-phosphotyrosine antibody 4G10.

Cell Proliferation Assays

Proliferation was measured by plating 5×10^4 U251 cells/well of six-well plates and counting the cells every 2 days. At day 1, for treated wells, 10 μmol/L PP2 or 5 μmol/L SU6656 were added. The medium containing the inhibitors was replaced every 2 days.

The proliferative population of U251 was determined by indirect immunofluorescence against the nuclear protein Ki67. Briefly, cells treated for 4 days with the PP2 or PP3 inhibitors were fixed 15 minutes in 4% paraformaldehyde, permeabilized with 0.1% Triton/PBS, and blocked 45 minutes in 0.5 % bovine serum albumin in PBS. The cells were then incubated for 1 hour with anti-Ki67 (1:200, PharMingen, San Diego, CA), washed, and incubated with Cy3-labeled goat anti-mouse antibodies (1:400, Jackson ImmunoResearch, West Grove, PA). Before mounting and examination by fluorescence microscopy, the cells were counterstained for 2 minutes with Hoechst 33258 (Sigma, St. Louis, MO).

Recombinant Adenoviruses

The DN and activated Src adenoviruses used in this study have been described previously (17). The CSK adenovirus was obtained using the same method, the pAdEasy recombination system (Stratagene, La Jolla, CA; 51). The rat CSK cDNA was a generous gift from Dr. Jean-François Côté (McGill University, Montreal, Quebec, Canada). Briefly, CSK was cloned in the GFP-expressing shuttle vector pAdTrack, recombined with the adenoviral vector pAdEasy by co-electroporation in bacteria, linearized, transfected, and amplified in 293A cells. The viruses were purified by centrifugation on CsCl gradients, dialyzed, and titered in 293A cells.

The invasion distance assay described above was modified the following way: Prior to implantation into the collagen matrix, the U251 spheroids were incubated with 10^6 plaque-forming units of the respective viruses in 1 mL complete DMEM for a few hours. The viruses are then washed and the spheroid was implanted. After 24 hours, a GFP image of the spheroid is taken and saved. A movie is then taken and the invasion distances of individual cells were measured as described above. When all the numbers have been compiled, the GFP image is overlaid on the first phase image of the movie to determine which of the cells were infected and the results were allocated accordingly.

YFP-Actin U251 Cells

The actin cytoskeleton of live U251 cells was imaged using the pEYFP-actin construct from Clontech (Palo Alto, CA). The construct was transfected using LipofectAMINE Plus (Invitrogen, Gaithersburg, MD) in U251 cells, which were then selected in 0.6 mg/mL G418 (Life Technologies, Gaithersburg, MD) until clones could be seen. Three clones expressing high amounts of YFP-actin, as seen under fluorescence microscopy, were isolated and expanded. Movies in two and three dimensions were made, taking pictures every 30 seconds of the same cells before and after addition of the PP2 inhibitor. For monolayers, the cells were placed without cover in the conditioned chamber of the microscope in a minimal amount of complete DMEM. At time 0, the volume is doubled with prewarmed complete DMEM containing the inhibitor at a 2× concentration. For collagen gels, the medium overlaying the gel is removed before the beginning of the movie. The plate is placed without cover on the microscope, and at time 0, 500 μL prewarmed complete DMEM containing the inhibitor at 2× concentration is pipetted onto the gel.

Acknowledgments

We thank Drs. Joan Brugge and Jean-François Côté for the generous gifts of the Src antibody and CSK cDNA, respectively, and A-M. Osiceanu for critical reading of the article.

References

1. Castro MG, Cowen R, Williamson IK, et al. Current and future strategies for the treatment of malignant brain tumors. Pharmacol Ther 2003;98:71–108.

2. Del Maestro RF, Shivers R, McDonald W, Del Maestro AG. Dynamics of C6 astrocytoma invasion into three-dimensional collagen gels. J Neurooncol 2001; 53:87–98.

3. Bauman GS, Fisher BJ, McDonald W, Amberger VR, Moore E, Del Maestro RF. Effects of radiation on a three-dimensional model of malignant glioma invasion. Int J Dev Neurosci 1999;17:643–51.

4. Tamaki M, McDonald W, Amberger VR, Moore E, Del Maestro RF. Implantation of C6 astrocytoma spheroid into collagen type I gels: invasive, proliferative, and enzymatic characterizations. J Neurosurg 1997;87:602–9.

5. Del Duca D, Werbowetski T, Del Maestro RF. Spheroid preparation from hanging drops: characterization of a model of brain tumor invasion. J Neurooncol 2004;67:295–303.

6. Friedl P, Wolf K. Tumor-cell invasion and migration: diversity and escape mechanisms. Nat Rev Cancer 2003;3:362–74.

7. Corcoran A, Del Maestro RF. Testing the "Go or Grow" hypothesis in human medulloblastoma cell lines in two and three dimensions. Neurosurgery 2003;53:174–84.

8. Sahai E, Marshall CJ. Differing modes of tumor cell invasion have distinct requirements for Rho/ROCK signaling and extracellular proteolysis. Nat Cell Biol 2003;5:711–9.

9. Tanaka Y, Kobayashi H, Suzuki M, Kanayama N, Terao T. Transforming growth factor-β1-dependent urokinase up-regulation and promotion of invasion are involved in Src-MAPK-dependent signaling in human ovarian cancer cells. J Biol Chem 2004;279:8567–76.

10. Recchia I, Rucci N, Festuccia C, et al. Pyrrolopyrimidine c-Src inhibitors reduce growth, adhesion, motility and invasion of prostate cancer cells *in vitro*. Eur J Cancer 2003;39:1927–35.

11. Boyd DD, Wang H, Avila H, et al. Combination of an SRC kinase inhibitor with a novel pharmacological antagonist of the urokinase receptor diminishes *in vitro* colon cancer invasiveness. Clin Cancer Res 2004;10:1545–55.

12. Hanke JH, Gardner JP, Dow RL, et al. Discovery of a novel, potent, and Src family-selective tyrosine kinase inhibitor. Study of Lck- and FynT-dependent T cell activation. J Biol Chem 1996;271:695–701.

13. Liu Y, Bishop A, Witucki L, et al. Structural basis for selective inhibition of Src family kinases by PP1. Chem Biol 1999;6:671–8.

14. Westermark B, Heldin CH, Nister M. Platelet-derived growth factor in human glioma. Glia 1995;15:257–63.

15. Blake RA, Broome MA, Liu X, et al. SU6656, a selective src family kinase inhibitor, used to probe growth factor signaling. Mol Cell Biol 2000;20:9018–27.

16. Singh SK, Clarke ID, Hide T, Dirks PB. Cancer stem cells in nervous system tumors. Oncogene 2004;23:7267–73.

17. Popsueva A, Poteryaev D, Arighi E, et al. GDNF promotes tubulogenesis of GFRα1-expressing MDCK cells by Src-mediated phosphorylation of Met receptor tyrosine kinase. J Cell Biol 2003;161:119–29.

18. Brown DC, Gatter KC. Ki67 protein: the immaculate deception? Histopathology 2002;40:2–11.

19. Okada M, Nada S, Yamanashi Y, Yamamoto T, Nakagawa H. CSK: a protein-tyrosine kinase involved in regulation of src family kinases. J Biol Chem 1991; 266:24249–52.

20. Senger DL, Tudan C, Guiot MC, et al. Suppression of Rac activity induces apoptosis of human glioma cells but not normal human astrocytes. Cancer Res 2002;62:2131–40.

21. Cary LA, Klinghoffer RA, Sachsenmaier C, Cooper JA. SRC catalytic but not scaffolding function is needed for integrin-regulated tyrosine phosphorylation, cell migration, and cell spreading. Mol Cell Biol 2002;22:2427–40.

22. Kaplan KB, Swedlow JR, Morgan DO, Varmus HE. c-Src enhances the spreading of src−/− fibroblasts on fibronectin by a kinase-independent mechanism. Genes Dev 1995;9:1505–17.

23. Rosenfeldt HM, Hobson JP, Maceyka M, et al. EDG-1 links the PDGF receptor to Src and focal adhesion kinase activation leading to lamellipodia formation and cell migration. FASEB J 2001;15:2649–59.

24. Vouret-Craviari V, Bourcier C, Boulter E, van Obberghen-Schilling E. Distinct signals via Rho GTPases and Src drive shape changes by thrombin and sphingosine-1-phosphate in endothelial cells. J Cell Sci 2002;115:2475–84.

25. Westphal M, Jungbluth A, Heidecker M, et al. Microfilament dynamics during cell movement and chemotaxis monitored using a GFP-actin fusion protein. Curr Biol 1997;7:176–83.

26. Yeatman TJ. A renaissance for SRC. Nat Rev Cancer 2004;4:470–80.

27. Martin GS. The hunting of the Src. Nat Rev Mol Cell Biol 2001;2:467–75.

28. Thomas SM, Brugge JS. Cellular functions regulated by Src family kinases. Annu Rev Cell Dev Biol 1997;13:513–609.

29. Werbowetski T, Bjerkvig R, Del Maestro RF. Evidence for a secreted chemorepellent that directs glioma cell invasion. J Neurobiol 2004;60:71–88.

30. Bjerkvig R, Laerum OD, Mella O. Glioma cell interactions with fetal rat brain aggregates *in vitro* and with brain tissue *in vivo*. Cancer Res 1986;46: 4071–9.

31. Nygaard SJ, Pedersen PH, Mikkelsen T, Terzis AJ, Tysnes OB, Bjerkvig R. Glioma cell invasion visualized by scanning confocal laser microscopy in an *in vitro* co-culture system. Invasion Metastasis 1995;15:179–88.

32. Engebraaten O, Bjerkvig R, Lund-Johansen M, et al. Interaction between human brain tumor biopsies and fetal rat brain tissue *in vitro*. Acta Neuropathol (Berl) 1990;81:130–40.

33. Boyer B, Bourgeois Y, Poupon MF. Src kinase contributes to the metastatic spread of carcinoma cells. Oncogene 2002;21:2347–56.

34. Slack JK, Adams RB, Rovin JD, Bissonette EA, Stoker CE, Parsons JT. Alterations in the focal adhesion kinase/Src signal transduction pathway correlate with increased migratory capacity of prostate carcinoma cells. Oncogene 2001;20: 1152–63.

35. Tapon N, Hall A. Rho, Rac and Cdc42 GTPases regulate the organization of the actin cytoskeleton. Curr Opin Cell Biol 1997;9:86–92.

36. Klemke RL, Leng J, Molander R, Brooks PC, Vuori K, Cheresh DA. CAS/Crk coupling serves as a "molecular switch" for induction of cell migration. J Cell Biol 1998;140:961–72.

37. Brugnera E, Haney L, Grimsley C, et al. Unconventional Rac-GEF activity is mediated through the Dock180-ELMO complex. Nat Cell Biol 2002;4:574–82.

38. Cote JF, Vuori, K. Identification of an evolutionarily conserved superfamily of DOCK180-related proteins with guanine nucleotide exchange activity. J Cell Sci 2002;115:4901–13.

39. Scaife RM, Courtneidge SA, Langdon WY. The multi-adaptor proto-oncoprotein Cbl is a key regulator of Rac and actin assembly. J Cell Sci 2003; 116:463–73.

40. Roth W, Wild-Bode C, Platten M, et al. Secreted Frizzled-related proteins inhibit motility and promote growth of human malignant glioma cells. Oncogene 2000;19:4210–20.

41. Giese A, Loo MA, Tran N, Haskett D, Coons SW, Berens ME. Dichotomy of astrocytoma migration and proliferation. Int J Cancer 1996;67:275–82.

42. Merzak A, McCrea S, Koocheckpour S, Pilkington GJ. Control of human glioma cell growth, migration and invasion *in vitro* by transforming growth factor β1. Br J Cancer 1994;70:199–203.

43. Kunapuli P, Chitta KS, Cowell JK. Suppression of the cell proliferation and invasion phenotypes in glioma cells by the LGI1 gene. Oncogene 2003;22: 3985–91.

44. Kim SK, Wang KC, Cho BK, et al. Adenoviral p16/CDKN2 gene transfer to malignant glioma: role of p16 in growth, invasion, and senescence. Oncol Rep 2003;10:1121–6.

45. MacFarlane SN, Sontheimer H. Modulation of Kv1.5 currents by Src tyrosine phosphorylation: potential role in the differentiation of astrocytes. J Neurosci 2000;20:5245–53.

46. Giese A, Bjerkvig R, Berens ME, Westphal M. Cost of migration: invasion of malignant gliomas and implications for treatment. J Clin Oncol 2003;21: 1624–36.

47. Yanamandra N, Berhow MA, Konduri S, et al. Triterpenoids from Glycine max decrease invasiveness and induce caspase-mediated cell death in human SNB19 glioma cells. Clin Exp Metastasis 2003;20:375–83.

48. Tatter SB, Shaw EG, Rosenblum ML, et al. An inflatable balloon catheter and liquid ^{125}I radiation source (GliaSite Radiation Therapy System) for treatment of recurrent malignant glioma: multicenter safety and feasibility trial. J Neurosurg 2003;99:297–303.

49. Zagzag D, Nomura M, Friedlander DR, et al. Geldanamycin inhibits migration of glioma cells *in vitro*: a potential role for hypoxia-inducible factor (HIF-1α) in glioma cell invasion. J Cell Physiol 2003;196:394–402.

50. Kennedy TE, Serafini T, de la Torre JR, Tessier-Lavigne M. Netrins are diffusible chemotropic factors for commissural axons in the embryonic spinal cord. Cell 1994;78:425–35.

51. He TC, Zhou S, da Costa LT, Yu J, Kinzler KW, Vogelstein B. A simplified system for generating recombinant adenoviruses. Proc Natl Acad Sci U S A 1998; 95:2509–14.